Inorg. Chem. **2009**, *48*, 3875−3881

Inorganic Chemistry
Article

DFT Study on N_2 Activation by a Hydride-Bridged Diniobium Complex. $N\equiv N$ Bond Cleavage Accompanied by H_2 Evolution

Hiromasa Tanaka,[†] Yoshihito Shiota,[†] Tsukasa Matsuo,[‡] Hiroyuki Kawaguchi,[*,§] and Kazunari Yoshizawa[*,†]

Institute for Materials Chemistry and Engineering, Kyushu University, Fukuoka, Japan 819-0395,
Functional Elemento-Organic Chemistry Unit, RIKEN, Wako, Saitama, Japan 351-0198, and
Department of Chemistry, Tokyo Institute of Technology, Ookayama, Meguro-ku, Tokyo,
Japan 152-8551

Received December 13, 2008

Density functional theory (DFT) calculations have been performed for the investigation of a plausible mechanism of the triple bond cleavage of N_2 in a diniobium complex supported by tridentate aryloxide ligands, $\{Nb^V(\mu\text{-}N)_2Nb^V\}^{2-}$.[22] With the assumption of a tetrakis(μ-hydrido)diniobium complex $\{Nb^{IV}(\mu\text{-}H)_4Nb^{IV}\}^{2-}$ as an initial complex, the $N\equiv N$ cleavage on the Nb_2 core proceeds in four steps. Dinitrogen is coordinated to the $\{Nb^{III}(\mu\text{-}H)_2Nb^{III}\}$ core in a side-on/end-on manner, accompanied by the reductive elimination of H_2. The $N\equiv N$ bond of dinitrogen is activated up to a single bond (formally N_2^{4-}) by the two Nb(III) atoms, once it is bound to the Nb_2 core. Two electrons are prepared for the cleavage of the N−N single bond through the μ-H migration to an N atom, leading to the formation of an Nb−Nb bond. The N−N bond is then dissociated by the two electrons that are shared between the two Nb atoms. Finally, $\{Nb(\mu\text{-}N)_2Nb\}^{2-}$ is generated after H_2 elimination in which the N-bonded H atom is coupled with the remaining μ-H atom. The final H_2 elimination is calculated to be the rate-determining step.

1. Introduction

Dinitrogen activation and its functionalization under mild conditions are challenging topics in synthetic chemistry and catalysis.[1] Dinitrogen is abundant in the atmosphere, but its high thermodynamic stability makes it extremely inert. At present, there are a number of metal complexes that are able to cleave the $N\equiv N$ triple bond to form well-characterized nitride compounds[2−12] or to generate ammonia catalytically in the presence of a pair of proton/electron sources.[13,14] In such nitride compound formation reported to date, N_2 scission relies on strongly reducing early transition/f-element metals as well as formation of a very strong metal-nitride linkage. This type of transformation very often implicates the reduction of a high oxidation metal halide with an alkali metal.[12,15−17] One important direction of this research is the search for new metal complexes capable of activating N_2 and eventually cleaving it.[12,15−18] There is much current interest in the activation of N_2 by hydride complexes, because this process plays a crucial role in developing the catalytic conversion of N_2 into NH_3 through hydrogenation.[19,20] Metal hydride species could be reactive intermediates in the catalytic cycle of the enzyme nitrogenase.[21]

We have shown that niobium complexes supported by triaryloxide ligands display the ability to split dinitrogen. Treatment of $[(L)NbCl_2]_2$ (**1**; L^{3-} as shown in Chart 1) with $LiBH(C_2H_5)_3$ under N_2 gave the nitride complex $[(L)Nb(\mu\text{-}N)Li(thf)]_2$ (**2**).[22] We expect that the reaction proceeds

---

[*] To whom correspondence should be addressed. E-mail: hkawa@chem.titech.ac.jp (H.K.), kazunari@ms.ifoc.kyushu-u.ac.jp (K.Y.).

[†] Kyushu University.

[‡] RIKEN.

[§] Tokyo Institute of Technology.

(1) (a) MacLachlan, E. A.; Fryzuk, M. D. *Organometallics* **2006**, *25*, 1530. (b) Himmel, H.-J.; Reiher, M. *Angew. Chem., Int. Ed.* **2006**, *45*, 6264.

(2) Mindiola, D. J.; Meyer, K.; Cherry, J.-P. F.; Baker, T. A.; Cummins, C. C. *Organometallics* **2000**, *19*, 1622.

(3) Clentsmith, G. K. B.; Bates, V. M. E.; Hitchcock, P. B.; Cloke, F. G. N. *J. Am. Chem. Soc.* **1999**, *121*, 10444.

(4) Caselli, A.; Solari, E.; Scopelliti, R.; Floriani, C.; Re, N.; Rizzoli, C.; Chiesi-Villa, A. *J. Am. Chem. Soc.* **2000**, *122*, 3652.

(5) (a) Korobkov, I.; Gambarotta, S.; Yap, G. P. A. *Angew. Chem., Int. Ed.* **2002**, *41*, 3433. (b) Korobkov, I.; Gambarotta, S.; Yap, G. P. A. *Angew. Chem., Int. Ed.* **2003**, *42*, 814. (c) Ilango, S.; Vidjayacoumar, B.; Gambarotta, S.; Gorelsky, S. I. *Inorg. Chem.* **2008**, *47*, 3265.

(6) (a) Fryzuk, M. D.; Kozak, C. M.; Bowdridge, M. R.; Patrick, B. O.; Rettig, S. J. *J. Am. Chem. Soc.* **2002**, *124*, 8389. (b) Morello, L.; Yu, P.; Carmichael, C. D.; Patrick, B. O.; Fryzuk, M. D. *J. Am. Chem. Soc.* **2005**, *127*, 12796.

10.1021/ic802377p CCC: $40.75

Chart 1. Aryloxide Ligands L^{3-} and L'^{3-}

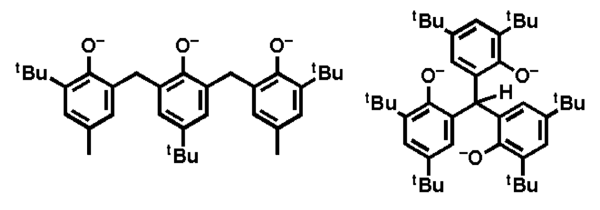

L^{3-} L'^{3-}

through a diniobium hydride intermediate that binds and cleaves dinitrogen via the elimination of H_2. A diniobium species analogous to the proposed hydride diniobium intermediate that is supported instead by a tripodal triaryloxide ligand (L′) has been reported recently. Indeed, the tetrakis(μ-hydrido) binuclear complex $[(L')Nb(\mu\text{-}H)_2K(dme)]_2$ is found to lose H_2 upon exposure to N_2 and split the N≡N triple bond, yielding $[(L')Nb(\mu\text{-}N)K(thf)_2]_2$.[23] In these reactions, six electrons required to convert N≡N to two N^{3-} groups are apparently provided by the reductive eliminations of hydride ligands as H_2 and the Nb−Nb metal bond. However, the detailed mechanism of N_2 activation by the hydride complexes is not clear.

Computational chemistry has provided valuable insights into our understanding of the binding of dinitrogen to binuclear transition metal complexes and the bonding nature between metal and dinitrogen.[24−31] A limited number of computational studies on bimetallic dinitrogen complexes have been reported on the mechanism of N_2 cleavage as well as the hydrogenation of the N_2 ligand. To our knowledge, the mechanism of the N≡N cleavage by a three-coordinate Mo complex reported by Cummins and co-workers[9] was theoretically investigated by Morokuma and co-workers,[32,33] Rösch and co-workers,[34] Stranger and co-workers,[35] and Yates and co-workers.[36] Reiher and co-workers[37] theoretically investigated the diprotonation of a binuclear ruthenium N_2 complex prepared by Sellmann and co-workers.[38] Morokuma and co-workers[39] reported density functional theory (DFT) studies on the hydrogenation of a binuclear zirconium N_2 complex prepared by Fryzuk and co-workers.[19] Another contribution to clarifying the reaction mechanism of a bimetallic N_2 complex with H_2 has been made by Hirao and co-workers[40] on a binuclear zirconium N_2 complex with the η^5-C_5Me_4H ligands prepared by Chirik and co-workers.[8] The reactivity of Ti and Hf analogues with H_2 were theoretically investigated by Musaev, Morokuma, and co-workers.[41] However, we have no good knowledge about how a bimetallic core and hydrides cooperate to cleave the strong triple bond of N_2. Elucidating the mechanism of the N≡N bond cleavage at a bimetallic hydride core is a fascinating subject, because the mandatory evolution of H_2 in the enzymatic N_2 fixation process[21] might be relevant to the evolution of H_2 observed in the formation of our bis(μ-

---

(7) Hirotsu, M.; Fontaine, P. P.; Epshteyn, A.; Zavalij, P. Y.; Sita, L. R. *J. Am. Chem. Soc.* **2007**, *129*, 9284.
(8) Pool, J. A.; Lobkovsky, E.; Chirik, P. J. *Nature* **2004**, *427*, 527.
(9) (a) LaPlaza, C. E.; Cummins, C. C. *Science* **1995**, *268*, 861. (b) Curley, J. J.; Cook, T. R.; Reece, S. Y.; Müller, P.; Cummins, C. C. *J. Am. Chem. Soc.* **2008**, *130*, 9394.
(10) Solari, E.; Da Silva, C.; Iacono, B.; Hesschenbrouck, J.; Rizzoli, C.; Scopelliti, R.; Floriani, C. *Angew. Chem., Int. Ed.* **2001**, *40*, 3907.
(11) (a) MacKay, B. A.; Munha, R. F.; Fryzuk, M. D. *J. Am. Chem. Soc.* **2006**, *128*, 9472. (b) MacKay, B. A.; Johnson, S. A.; Patrick, B. O.; Fryzuk, M. D. *Can. J. Chem.* **2005**, *83*, 315. (c) Fryzuk, M. D.; MacKay, B. A.; Johnson, S. A.; Patrick, B. O. *Angew. Chem., Int. Ed.* **2002**, *41*, 3709. (d) Fryzuk, M. D.; MacKay, B. A.; Patrick, B. O. *J. Am. Chem. Soc.* **2003**, *125*, 3234. (e) MacKay, B. A.; Patrick, B. O.; Fryzuk, M. D. *Organometallics* **2005**, *24*, 3836.
(12) Tsai, Y.-C.; Johnson, M. J. A.; Mindiola, D. J.; Cummins, C. C. *J. Am. Chem. Soc.* **1999**, *121*, 10426.
(13) (a) Yandulov, D. V.; Schrock, R. R. *J. Am. Chem. Soc.* **2002**, *124*, 6252. (b) Yandulov, D. V.; Schrock, R. R. *Science* **2003**, *301*, 76. (c) Schrock, R. R. *Angew. Chem., Int. Ed.* **2008**, *47*, 5512.
(14) (a) Cao, Z.; Zhou, Z.; Wan, H.; Zhang, Q. *Int. J. Quantum Chem.* **2005**, *103*, 344. (b) Studt, F.; Tuczek, F. *Angew. Chem., Int. Ed.* **2005**, *44*, 5639. (c) Le Guennic, B.; Kirchner, B.; Reiher, M. *Chem.−Eur. J.* **2005**, *11*, 7448. (c) Reiher, M.; Le Guennic, B.; Kirchner, B. *Inorg. Chem.* **2005**, *44*, 9640. (d) Magistrato, A.; Robertazzi, A.; Carloni, P. *J. Chem. Theory Comput.* **2007**, *3*, 1708. (e) Schenk, S.; Le Guennic, B.; Kirchner, B.; Reiher, M. *Inorg. Chem.* **2008**, *47*, 3634.
(15) Fryzuk, M. D.; Johnson, S. A.; Rettig, S. J. *J. Am. Chem. Soc.* **1998**, *120*, 11024.
(16) Chirik, P. J.; Henling, L. M.; Bercaw, J. E. *Organometallics* **2001**, *20*, 534.
(17) Fout, A. R.; Basuli, F.; Fan, H.; Tomaszewski, J.; Huffman, J. C.; Baik, M.-H.; Mindiola, D. J. *Angew. Chem., Int. Ed.* **2006**, *45*, 3291.
(18) Pun, D.; Lobkovsky, E.; Chirik, P. J. *J. Am. Chem. Soc.* **2008**, *130*, 6047.
(19) Fryzuk, M. D.; Love, J. B.; Rettig, S. J.; Young, V. G. *Science* **1997**, *275*, 1445.
(20) Avernier, P.; Taiufil, M.; Lesage, A.; Solans-Monfort, X.; Baudouin, A.; de Mallmann, A.; Veyre, L.; Basset, L.-M.; Eisenstein, O.; Emsley, L.; Quadrelli, E. A. *Science* **2007**, *317*, 1056.
(21) (a) Sadique, A. R.; Gregory, E. A.; Brennessel, W. W.; Holland, P. L. *J. Am. Chem. Soc.* **2007**, *129*, 8112. (b) Eady, R. R. *Chem. Rev.* **1996**, *96*, 3013.
(22) Kawaguchi, H.; Matsuo, T. *Angew. Chem., Int. Ed.* **2002**, *41*, 2792.
(23) Akagi, F.; Matsuo, T.; Kawaguchi, H. *Angew. Chem., Int. Ed.* **2007**, *46*, 8778.
(24) Goldberg, K.; Hoffman, D. M.; Hoffmann, R. *Inorg. Chem.* **1982**, *21*, 3863.
(25) Powell, C. B.; Hall, M. B. *Inorg. Chem.* **1984**, *23*, 4619.
(26) Pelikán, P.; Boča, R. *Coord. Chem. Rev.* **1984**, *55*, 55.
(27) Fryzuk, M. D.; Haddad, T. S.; Mylvaganam, M.; McConville, D. H.; Rettig, S. J. *J. Am. Chem. Soc.* **1993**, *115*, 2782.
(28) Fryzuk, M. D.; Johnson, S. A.; Patrick, B. O.; Albinati, A.; Mason, S. A.; Koetzle, T. F. *J. Am. Chem. Soc.* **2001**, *123*, 3960.
(29) Bobadova-Parvanova, P.; Wang, Q.; Morokuma, K.; Musaev, D. G. *Angew. Chem., Int. Ed.* **2005**, *44*, 7101.
(30) Studt, F.; Tuczek, F. *J. Comput. Chem.* **2006**, *27*, 1278.
(31) Himmel, H.-J.; Reiher, M. *Angew. Chem., Int. Ed.* **2006**, *45*, 6264.
(32) Cui, Q.; Musaev, D. G.; Svensson, M.; Sieber, S.; Morokuma, K. *J. Am. Chem. Soc.* **1995**, *117*, 12366.
(33) Khoroshun, D. V.; Musaev, D. G.; Morokuma, K. *Organometallics* **1999**, *18*, 5653.
(34) Neyman, K. M.; Nasluzov, V. A.; Hahn, J.; Landis, C. R.; Rösch, N. *Organometallics* **1997**, *16*, 995.
(35) Christian, G.; Driver, J.; Stranger, R. *Faraday Discuss.* **2003**, *124*, 331.
(36) Graham, D. C.; Beran, G. J. O.; Head-Gordon, M.; Christian, G.; Stranger, R.; Yates, B. F. *J. Phys. Chem. A* **2005**, *109*, 6762.
(37) (a) Reiher, M.; Salomon, O.; Sellmann, D.; Hess, B. A. *Chem.−Eur. J.* **2001**, *7*, 5195. (b) Reiher, M.; Kirchner, B.; Hutter, J.; Sellmann, D.; Hess, B. A. *Chem.−Eur. J.* **2004**, *10*, 4443. (c) Kirchner, B.; Reiher, M.; Hille, A.; Hutter, J.; Hess, B. A. *Chem.−Eur. J.* **2005**, *11*, 574.
(38) Sellmann, D.; Hille, A.; Rösler, A.; Heinemann, F. W.; Moll, M.; Brehm, G.; Schneider, S.; Reiher, M.; Hess, B. A.; Bauer, W. *Chem.−Eur. J.* **2004**, *10*, 819.
(39) (a) Basch, H.; Musaev, D. G.; Morokuma, K.; Fryzuk, M. D.; Love, J. B.; Seidel, W. W.; Albinati, A.; Koetzle, T. F.; Klooster, W. T.; Mason, S. A.; Eckert, J. *J. Am. Chem. Soc.* **1999**, *121*, 523. (b) Basch, H.; Musaev, D. G.; Morokuma, K. *J. Am. Chem. Soc.* **1999**, *121*, 5754. (c) Yates, B. F.; Basch, H.; Musaev, D. G.; Morokuma, K. *J. Chem. Theory Comput.* **2006**, *2*, 1298.
(40) Miyachi, H.; Shigeta, Y.; Hirao, K. *J. Phys. Chem. A* **2005**, *109*, 8800.
(41) (a) Musaev, D. G.; Bobadova-Parvanova, P.; Morokuma, K. *Inorg. Chem.* **2007**, *46*, 2709. (b) Martinez, S.; Morokuma, K.; Musaev, D. G. *Organometallics* **2007**, *26*, 5978.

Scheme 1. Synthesis of {Nb(μ-N)$_2$Nb} Complex **2** by Reduction of **1**

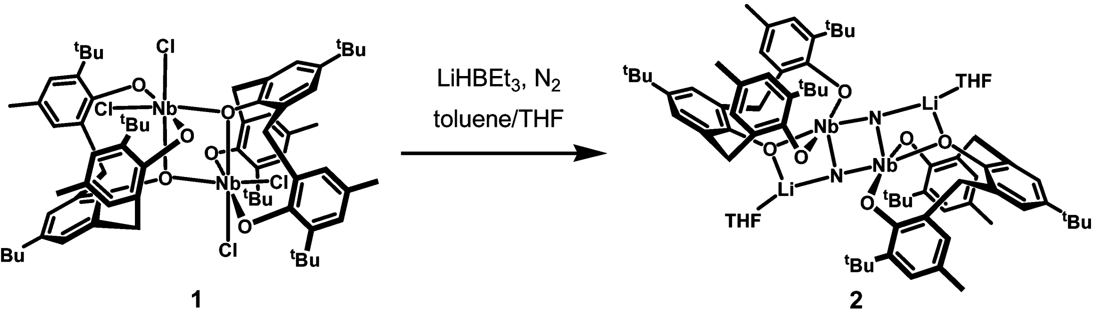

Scheme 2. Proposed Mechanism of the N≡N Bond Cleavage Starting with the Tetrakis(μ-hydrido)diniobium Complex **3**

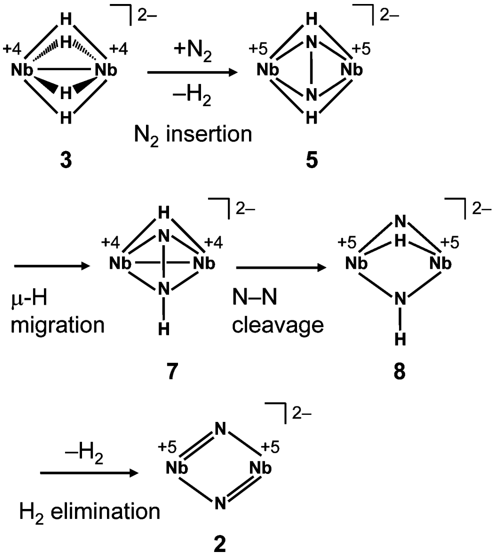

nitrido)diniobium complexes. In this paper, we describe DFT calculations on a possible mechanism for the reaction presented in Scheme 2 starting from a proposed hydride intermediate.

2. Computational Method

We chose the tetrakis(μ-hydrido)diniobium complex **3**, having a bulky aryloxide ligand L^{3-} (Scheme 1), as an initial complex to investigate the formation of the bis(μ-nitrido)diniobium complex **2** from the reaction of **1** with $LiBH(C_2H_5)_3$ in the presence of dinitrogen (Scheme 2). Although **3** has not been neither observed nor isolated, several pieces of experimental evidence strongly suggest that a hydrogen-bridged diniobium complex plays a key role in the formation of **2**: (1) Niobium(III) and -(IV) complexes, having the linear triaryloxide ligands, do not react with dinitrogen. (2) A niobium complex, having the linear triaryloxide ligands, cannot be reduced to the Nb(II) state with $LiBH(C_2H_5)_3$. This means that the direct formation of **2** from a reduced intermediate $\{Nb^{II}Nb^{II}\}^{2-}$ does not occur. (3) The reduction of **1** with KC_8 does not give a dinitrogen complex. (4) The tetrakis(μ-hydrido)diniobium complex supported by the L′ ligand has been isolated by Kawaguchi and co-workers.[23] This complex reacts with dinitrogen to yield the corresponding bis(μ-nitrido)diniobium complex.

All calculations were carried out with the Jaguar 6.5 or 7.0 programs.[42] We searched local minima and saddle points on a potential energy surface to characterize reaction intermediates and transition structures at the B3LYP/LACVP* level of theory.[43,44] LACVP* represents a mixed basis set using the LanL2DZ relativistic effective core potential (RECP) for niobium atoms and the standard 6-31G(d) basis set for the other atoms. For the comparison of the hybrid B3LYP functional with another functional often used, single-point energy calculations with the BP86 functional[43,45] were carried out for all intermediates with the singlet-spin-state and transition-state structures optimized at the B3LYP/LACVP* level of theory. The energy profiles calculated with the B3LYP and BP86 functionals are similar and the difference in the height of activation barriers is at most 5.9 kcal/mol. Details of the comparison are presented in the Supporting Information. Bond formations and cleavages in reaction processes are analyzed with the Mayer-bond-order calculation.[46] The aryloxide ligand L^{3-} is included without any simplification, while two Li atoms and two THF molecules in the X-ray structure of **2** are omitted. As a result, the bis(μ-nitrido)diniobium complex **2** consists of 164 atoms, and intermediates **2**−**9** and transition-state structures connecting them have a total charge of −2.

3. Results and Discussion

With the assumption of the tetrakis(μ-hydrido)diniobium complex **3** as the initial complex, we propose that the N≡N bond cleavage of dinitrogen in the diniobium complex proceeds in four steps, as shown in Scheme 2: (i) the N_2 insertion into **3** which is accompanied by the reductive elimination of H_2, (ii) the μ-H atom migration to form an N−H bond, (iii) the N−N bond cleavage, and (iv) the H_2 elimination to form the final product **2**. The overall energy profile calculated on the basis of this mechanism is summarized in Figure 1. Calculated energies presented in this figure are relative to $^{\mathbf{1}}\mathbf{4}$ and include zero-point energy corrections. Optimized structures of the intermediates and transition-state structures are depicted in Figures 2 and 3,

---

(42) *Jaguar, version 6.5*; Schrödinger, LLC: New York, NY, 2005. *Jaguar, version 7.0*; Schrödinger, LLC: New York, NY, 2007.

(43) (a) Becke, A. D. *Phys. Rev. A* **1988**, *38*, 3098. (b) Becke, A. D. *J. Chem. Phys.* **1993**, *98*, 5648. (c) Lee, C.; Yang, W.; Parr, R. G. *Phys. Rev. B* **1988**, *37*, 785. (d) Stephens, P. J.; Devlin, F. J.; Chabalowski, C. F.; Frisch, M. J. *J. Phys. Chem.* **1994**, *98*, 11623.

(44) (a) Ditchfield, R.; Hehre, W. J.; Pople, J. A. *J. Chem. Phys.* **1971**, *54*, 724. (b) Hehre, W. J.; Ditchfield, R.; Pople, J. A. *J. Chem. Phys.* **1972**, *56*, 2257. (c) Hariharan, P. C.; Pople, J. A. *Theor. Chim. Acta* **1973**, *28*, 213. (d) Clark, T.; Chandrasekhar, J.; Spitznagel, G. W.; Schleyer, P. v. R. *J. Comput. Chem.* **1983**, *4*, 294. (e) Francl, M. M.; Petro, W. J.; Hehre, W. J.; Binkley, J. S.; Gordon, M. S.; DeFrees, D. J.; Pople, J. A. *J. Chem. Phys.* **1982**, *77*, 3654. (f) Hay, P. J.; Wadt, W. R. *J. Chem. Phys.* **1985**, *82*, 299.

(45) (a) Perdew, J. P.; Zunger, A. *Phys. Rev. B* **1981**, *23*, 5048. (b) Perdew, J. P. *Phys. Rev. B* **1986**, *33*, 8822. Perdew, J. P. Erratum. *Phys. Rev. B* **1986**, *34*, 7406.

(46) (a) Mayer, I. *Chem. Phys. Lett.* **1983**, *97*, 270. (b) Mayer, I. *Int. J. Quantum Chem.* **1984**, *26*, 131.

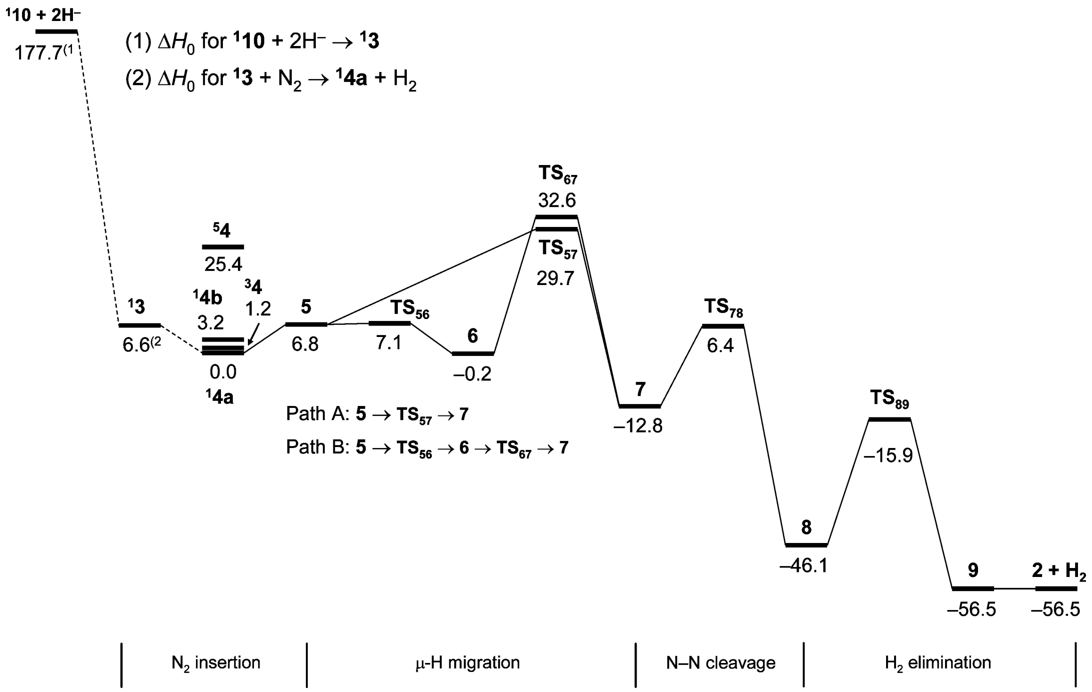

Figure 1. Energy diagram for the N≡N bond cleavage of dinitrogen by the tetrakis(*μ*-hydrido)diniobium complex **3** calculated at the B3LYP/LACVP+* level of theory. Energies in kcal/mol are relative to ^{1}**4a**, where zero-point energy corrections are included.

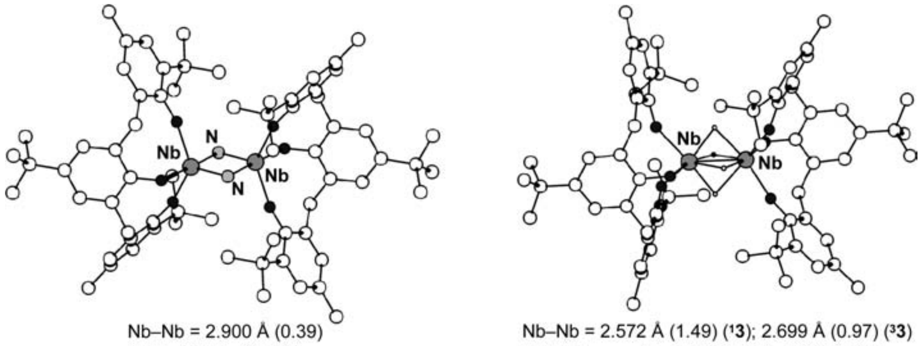

Nb–Nb = 2.900 Å (0.39)
N–N = 2.601 Å (0.00)

2

Nb–Nb = 2.572 Å (1.49) (^{1}**3**); 2.699 Å (0.97) (^{3}**3**)
Nb–H (average) = 1.955 Å (^{1}**3**); 1.971 Å (^{3}**3**)

3

Figure 2. Optimized structures of intermediates **2** and **3** calculated at the B3LYP/LACVP* level of theory. Mayer bond orders are presented in parentheses. Unlabeled black and white circles represent oxygen and carbon atoms, respectively. Small white circles in **3** represent hydrogen atoms, and the other hydrogen atoms are omitted for clarity.

together with selected geometric parameters and the Mayer bond orders.

N_2 Insertion into the {Nb(*μ*-H)$_4$Nb}$^{2-}$ Complex. The initial complex **3** contains two L^{3-} ligands and four hydrides, whose formal charges are −3 and −1, respectively. Because the formal charge of the two Nb atoms is counted to be +4, each Nb atom can contribute one d-electron to form an Nb−Nb bond. We therefore considered singlet and triplet spin states for **3**. As shown in Figure 2, the Nb−Nb distances and the Mayer bond orders (b.o.) suggest that the singlet ^{1}**3** has an Nb−Nb bonding interaction (Nb−Nb = 2.572 Å, b.o. = 1.49) stronger than the triplet ^{3}**3** (Nb−Nb = 2.702 Å, b.o. = 0.97). The singlet-state structure is 18.8 kcal/mol more stable than the triplet.

When dinitrogen is inserted into the diniobium core of **3**, a pair of the *μ*-H atoms has to be eliminated as an H_2 molecule to make space for the dinitrogen. This reductive elimination of H_2 results in the {Nb^{III}(*μ*-H)$_2$(*μ*-N$_2$)Nb^{III}}$^{2-}$ **4**. Singlet, triplet, and quintet spin states are considered for **4** because each Nb atom is able to contribute up to two d-electrons to dinitrogen. The singlet state of **4** has two stable structures, ^{1}**4a** and ^{1}**4b**. The dinitrogen in ^{1}**4a** and ^{1}**4b** is coordinated on the Nb$_2$ core in a side-on/end-on manner, and ^{1}**4a** is 3.2 kcal/mol more stable than ^{1}**4b**. The N−N distance in ^{1}**4a** is 1.264 Å, which is close to the value for diazene HN═NH (1.25 Å). The N−N distance as well as the N−N bond order (1.31) in ^{1}**4a** indicates that the triple bond of dinitrogen is activated up to a single or double bond. In other words, N_2 is reduced to be N_2^{2-} or N_2^{4-}, once it is bound to ^{1}**3**. A weak interaction is observed between the Nb atoms (Nb−Nb = 2.930 Å, b.o. = 0.81). On the other hand, the N−N distance and the N−N bond order in ^{1}**4b** are calculated to be 1.177 Å and 1.98, respectively. The Nb−Nb distance and the Nb−Nb bond order are 2.651 Å and 1.38, respectively, indicating that a strong bonding interaction remains between the two Nb atoms in ^{1}**4b**. The

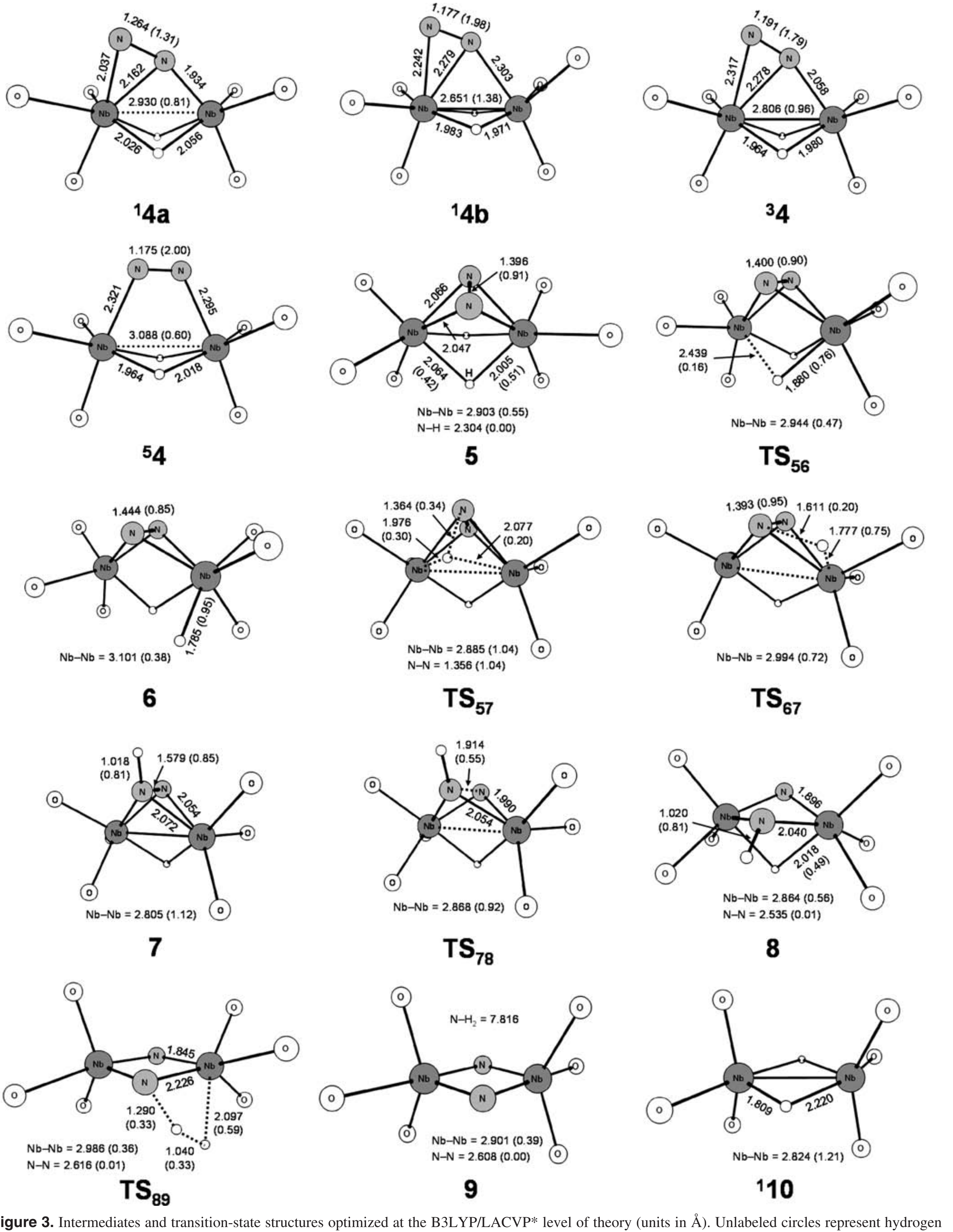

Figure 3. Intermediates and transition-state structures optimized at the B3LYP/LACVP* level of theory (units in Å). Unlabeled circles represent hydrogen atoms. Mayer bond orders are shown in parentheses. For the L^{3-} ligand, only oxygen atoms are described.

dinitrogen in ^{1}**4b** is reduced by less than two electrons. The interaction between the dinitrogen and the Nb_2 core is apparently stronger in ^{1}**4a**, which is responsible for the higher stability of ^{1}**4a**. The triplet state ^{3}**4** also binds dinitrogen in a side-on/end-on manner and is 1.2 kcal/mol less stable than the singlet state ^{1}**4a**. The longer Nb−Nb distance in ^{1}**4a** (2.930 Å) than in ^{3}**4** (2.806 Å) is due to the difference in the degree of N_2 activation and the strength of Nb−N bonding. The Nb−N distances in ^{1}**4a** are calculated to be 2.037 and 2.162 Å for Nb−η^2-N and 1.934 Å for Nb−η^1-N, which are much shorter than those in ^{3}**4**, 2.317 and 2.278 Å for Nb−η^2-N and 2.058 Å for Nb−η^1-N. Because the strongly activated N−N bond in ^{1}**4a** requires a strong Nb−N interaction, the N_2 ligand comes closer to the Nb_2 core and the Nb−Nb bond is increased in ^{1}**4a**. The quintet state ^{5}**4**, in which the dinitrogen is symmetrically coordinated to the two Nb atoms, is 25.4 kcal/mol less stable than ^{1}**4a**. The enthalpy change for the reaction ^{1}**3** + N_2 → ^{1}**4a** + H_2 is calculated to be −6.6 kcal/mol, indicating that the exchange of H_2 for N_2 undergoes in an exothermic way. For the side-on/end-on coordination of dinitrogen calculated for **4**, Fryzuk and co-workers reported the preparation of a bis(μ-hydrido)ditantalum complex ligating dinitrogen in a similar manner.[26] It is noteworthy that this dinitrogen complex is synthesized from a corresponding tetrakis(μ-hydrido)ditantalum complex under a mixture of N_2 and H_2 gas. In the X-ray structure of their dinitrogen complex, the N−N and Ta−Ta distances are, respectively, 1.319 and 2.830 Å, implying that the dinitrogen is reduced to be N^{2-} or N^{4-} by the Ta(μ-H)$_2$Ta core.

To connect the N_2 insertion step with the following reaction step, we have calculated intermediate **5**, in which dinitrogen is bound to the Nb atoms in a side-on/side-on manner. The formal charge of the Nb atoms in **5** is counted to be +5, and therefore we considered only the singlet state. The side-on/side-on coordination of dinitrogen is 6.8 kcal/mol less favorable than the side-on/end-on coordination. The N−N bond distance and the N−N bond order (1.396 Å and 0.91) suggest that N_2 is reduced by four electrons to be N_2^{4-}. The loss of the Nb−Nb bond (b.o. = 0.55) is associated with the four-electron reduction of dinitrogen. The higher stability of the side-on/end-on coordination is probably ascribed to the greater value of the Nb−Nb bond order. Because the Nb−Nb distance in the {Nb(μ-H)$_2$(μ-N)Nb} complex is kept close by the two μ-H atoms, the bonding interaction between the Nb atoms will provide an advantage in stability for the side-on/end-on coordination. A complete four-electron reduction of dinitrogen observed for the side-on/side-on coordination causes the loss of the Nb−Nb interaction.

As a possible mechanism of the formation of **2**, one might expect reductive elimination of H_2 from **4** or **5**. We searched this alternative pathway by partial optimizations while the distance between the two μ-H atoms were fixed. The two μ-H atoms are not attractive even when we approach the H atoms to less than 1.0 Å, and the partially optimized structures are relaxed to **4** or **5** once the H−H distance is not restrained. The calculational result suggests that H_2 elimination occurs as a result of proton-hydride coupling. This is a reason that we considered the next step (μ-H migration) after the N_2 insertion step.

N−H Bond Formation (μ-H Migration from Nb to N). Two additional electrons are required for the cleavage of the N−N single bond in **5**. However, the two Nb^{5+} atoms in **5** formally have no valence electron to break the N−N bond. If one of the μ-H atoms migrates to an N atom to form an N−H bond, the formal charge of the hydrogen atom is varied from −1 to +1, and thereby two electrons are prepared for the N−N bond cleavage. We discuss two possible pathways to reach intermediate **7** having one N-bonded H atom and one μ-H atom. In the first path (Path A), one of the μ-H atoms in **5** directly migrates to one of the N atoms to yield **7** via **TS$_{57}$**. In the second path (Path B), one of the bridging Nb−H bonds in **5** is first broken and intermediate **6** is formed via **TS$_{56}$**. The nonbridging H atom in **6** moves onto an adjacent N atom to give **7** via **TS$_{67}$**.

In the migration process along Path A, the N−H bond distance becomes shorter as the corresponding N−H bond order becomes larger, 2.304 Å (b.o. = 0.00) in **5**, 1.364 Å (0.34) in **TS$_{57}$**, and 1.018 Å (0.81) in **7**. Interestingly, a single bond is formed between the Nb atoms in **TS$_{57}$** (b.o. = 1.04) and **7** (1.12). This suggests that two electrons released from the μ-H atom are temporarily used for connecting the two Nb^{4+} atoms. We could not optimize any open-shell singlet structures of **7**, in which two Nb atoms are antiferromagnetically coupled, while the triplet-state structure is 6.0 kcal/mol less stable than the closed-shell singlet. The activation energy (E_a) for the direct μ-H migration is 22.9 kcal/mol. In Path B, breaking one of the bridging Nb−H bonds virtually proceeds as a barrierless reaction (E_a = 0.3 kcal/mol). Like in Path A, the N−H and Nb−Nb bonds are coincidentally formed in Path B. The N−H and Nb−Nb distances (bond orders) in **TS$_{67}$** are respectively 1.611 (0.20) and 2.994 Å (0.72), while the Nb−H bond is lost (b.o. = 0.95 (**6**) → 0.75 (**TS$_{67}$**)). The activation energy for **TS$_{67}$** is calculated to be 32.8 kcal/mol, which is greater than the value for **TS$_{57}$** (Path A).

We would like to comment on another pathway of μ-H migration starting from intermediate **4**, which has a side-on/end-on coordinated N_2. The result of partial optimizations (N···H distance fixed) show that the activation energy for the μ-H migration is greater than 40 kcal/mol. Therefore, we decided to exclude this pathway from consideration.

N−N Bond Cleavage. In the third step, the N−N single bond in **7** is cleaved to give **8** via **TS$_{78}$**. The N−N bond distances (bond orders) change from 1.579 Å (0.85) in **7** to 1.914 Å (0.56) in **TS$_{78}$**, and the N−N bond is completely cleaved in **8** (N−N = 2.535 Å). The difference in the Nb−Nb bond order among **7** (1.12), **TS$_{78}$** (0.92), and **8** (0.55) clearly shows that two electrons shared between the Nb atoms move to the N_2 moiety to break the N−N single bond, while the Nb−Nb distances are not significantly different in the three species: 2.805 Å (**7**) → 2.868 Å (**TS$_{78}$**) → 2.864 Å (**8**). The N−N single bond cleavage in the diniobium complex is highly exothermic (ΔH_0 = −33.3 kcal/mol) and requires an E_a of 19.2 kcal/mol.

H_2 Elimination and {Nb(μ-N)$_2$Nb}$^{2-}$ Formation. In the final step, the bridging H atom in **8** is coupled with the N-bonded H atom, leading to the elimination of an H_2

molecule and the formation of the bis(μ-nitrido)diniobium complex **2**. The shortening of the H−H distance in **8** causes a spontaneous cleavage of a bridging Nb−H bond and then results in the transition state $\mathbf{TS_{89}}$ (H−H = 1.040 Å, b.o. = 0.33). The activation barrier for the formation of H_2 is as high as 30.2 kcal/mol, which is the greatest value in all the transition states calculated in the present study if the N−H bond formation undergoes along Path A. This H_2 elimination is the rate-determining step in the N−N bond cleavage by the diniobium complex. The optimized structure of **2** reasonably reproduces the X-ray crystallographic structure, despite the lack of Li and THF. The calculated N−N and Nb−Nb distances (2.601 and 2.900 Å, respectively) are in good agreement with the experimental values (2.569 and 2.837 Å). Intermediate **9** is a complex of **2** and H_2, in which the H_2 molecule is loosely bound to **2**. The distance between the H_2 molecule and the nearest N atom is 7.816 Å, and the interaction between **2** and H_2 is negligibly weak (0.03 kcal/mol). Geometric parameters of the Nb(μ-N)$_2$Nb moiety in **9** are nearly identical to those of **2** (N−N = 2.608 Å, Nb−Nb = 2.901 Å). The generated bis(μ-nitrido)diniobium complex **2** shows poor reactivity with H_2. Oxidative addition of H_2 (**2** + H_2 → **8**) is endothermic ($\Delta H_0 = +10.4$ kcal/mol) and has a high activation barrier (40.6 kcal/mol). These values imply that the {Nb(μ-H)$_2$(μ-N)$_2$Nb} complex favors liberating H_2.

The overall reaction $\{Nb(\mu\text{-}H)_4Nb\}^{2-}$ (^{1}**3**) + N_2 → $\{Nb(\mu\text{-}N)_2Nb\}^{2-}$ (**2**) + 2H_2 is exothermic by −63.1 kcal/mol. The highest activation energy in the N≡N cleavage mechanism (30.2 kcal/mol) might be too large for a reaction occurring at room temperature. We could answer this problem if the neutral $\{Nb^{IV}(\mu\text{-}H)_2Nb^{IV}\}^0$ complex ^{1}**10** (Figure 2) exists as a precursor of ^{1}**3**. As shown in Figure 1, the enthalpy change for the reaction $\{Nb^{IV}(\mu\text{-}H)_2Nb^{IV}\}^0$ (^{1}**10**) + 2H^- → $\{Nb^{IV}(\mu\text{-}H)_4Nb^{IV}\}^{2-}$ (^{1}**3**) is −177.7 kcal/mol. The formation of ^{1}**3** from ^{1}**10** is extremely exothermic, and therefore one can expect that the generated **3** has a kinetic energy large enough to overcome all the energy barriers leading to **2**.

In conclusion, we have performed DFT calculations to propose a plausible mechanism of the dinitrogen-bond cleavage in the bis(μ-nitrido)diniobium complex **2**. With the assumption of the tetrakis(μ-hydrido)diniobium complex **3** as the initial complex, we demonstrated that the N−N cleavage proceeds in four steps. Accompanied by the reductive elimination of H_2, dinitrogen is coordinated to the diniobium core in a side-on/end-on manner. The N−N bond order in the N_2-coordinated complex is calculated to be nearly 1, implying that the coordinated dinitrogen is reduced by four electrons to be formally N_2^{4-}. In the next step, one of the two bridging μ-H atoms is migrated to an N atom to form an N−H bond. This μ-H migration supplies two electrons to the diniobium core resulting in the formation of an Nb−Nb bond. The N−N single bond is dissociated using two electrons temporary shared between the two Nb atoms. Finally, the second H_2 molecule is generated to give **3**, which is the rate-determining step in the N≡N bond cleavage mechanism. The Mayer bond order is found to be a powerful tool for understanding bond formations and cleavages in the reaction processes, while geometric parameters such as bond distances are not always sensitive to the changes in bonding nature. These calculational results strongly suggest that both the Nb−Nb bond and the bridging hydrides are utilized as a temporal electron reservoir in the reduction process of dinitrogen.

The calculational result that the H_2 elimination is exothermic indicates that it is difficult to stop the elimination once the N−N single bond is dissociated. In the μ-nidrido complex **2**, each Nb(V) center adopts a trigonal bipyramidal structure and its axial and equatorial positions are shared to form a planar Nb_2N_2 framework. The planar Nb_2N_2 framework appears to be energetically favorable because the L^{3-} ligands are symmetrically located along the axis connecting the two Nb atoms. A temporal formation of an Nb−Nb bond is essential in the proposed reaction mechanism while the planar Nb_2N_2 framework prevents the Nb−Nb bond formation. If the reaction stops at **7** having an Nb−Nb bond, functionalization of the nitrogen atoms might be possible. The Nb−Nb bond in **7** is ensured by a bridging hydride and is spontaneously broken when the Nb−H bond is dominated by a single Nb atom. A possible strategy for functionalization of the N atoms is to prepare a revised aryloxide ligand that forces a short Nb−Nb distance.

Acknowledgment. This work was supported by Grants-in-Aid for Scientific Research (Nos. 18350088, 18066013, 18064016, and 18GS0207) from the Japan Society for the Promotion of Science, the Nanotechnology Support Project of the Ministry of Culture, Sports, Science, and Technology of Japan (MEXT), the Joint Project of Chemical Synthesis Core Research Institutions of MEXT, and CREST of the Japan Science and Technology Cooperation.

Supporting Information Available: Comparison of energy profiles calculated with the B3LYP and BP86 functionals. Atomic Cartesian coordinates for all of the structures optimized in the present study. This material is available free of charge via the Internet at http://pubs.acs.org.

IC802377P